Equation of States in accretion and wind flows.

Soumen Mondal

Department of Physics, Jadavpur University, Kolkata.

In collaboration with Dr. Prasad Basu,

Cotton College State University, Guwahati, Assam.

The plan of the talk is the following :

(1): Fluid dynamics: A review of hydrodynamic solutions around a compact object with $\gamma = \frac{4}{3}$.

(2): The formation of shocks in accretion flows : e.g. SPH results, and its importance.

(3): The accretion and wind solution with variable adiabatic index ($\frac{4}{3} \leq \gamma \leq \frac{5}{3}$) and possibilities of shocks in the flow.

(4): Conclusions.

The spherical accretion ($l = 0$): Bondi accretion.

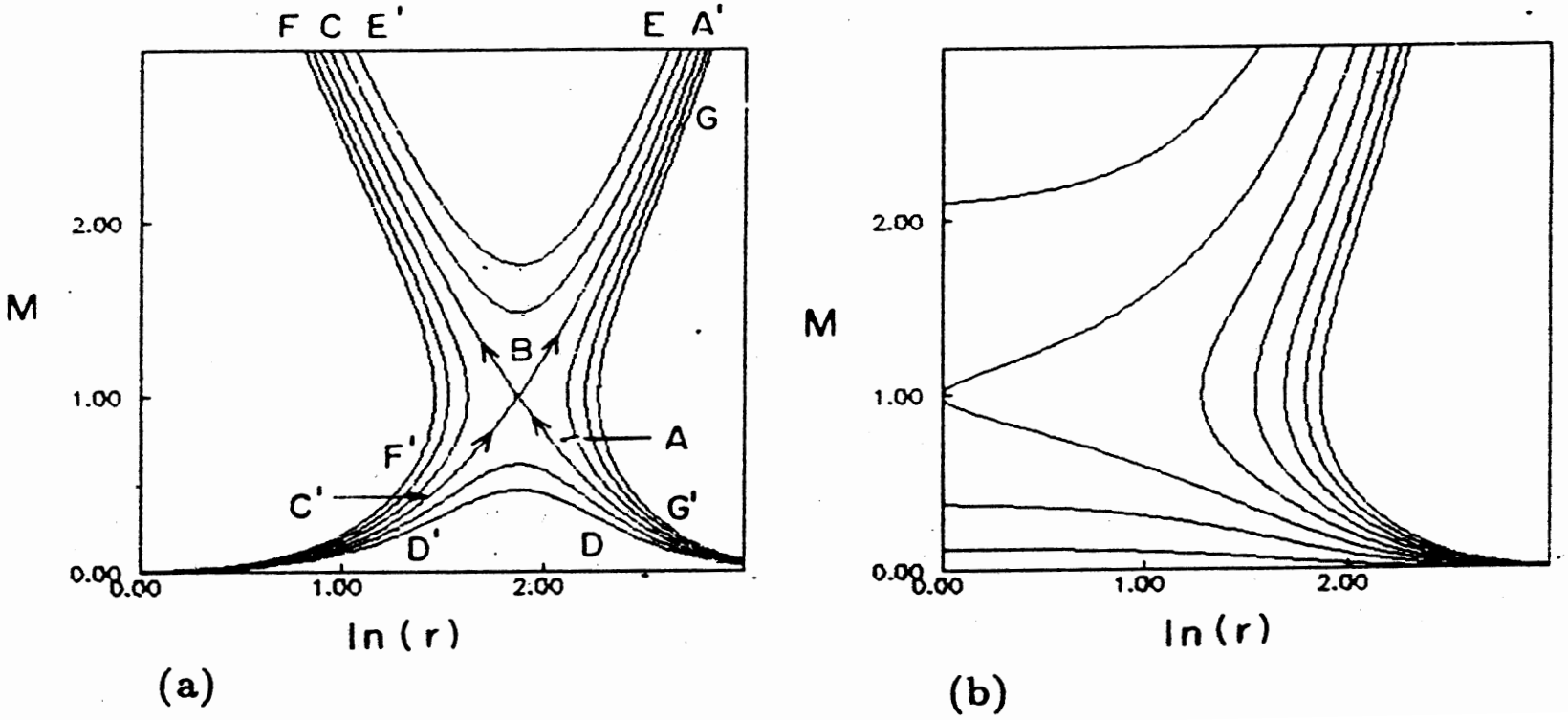

Bondi solutions (plots of Mach no. $M = \frac{v}{a_s}$ vs. radius) are shown. Number of sonic point is one.

(2) Boundary Conditions:

(i) Accretion: at $r \to \infty$, $v \to 0$ and at BH horizon, $v \to c$; at the NS surface, $v = 0$.

(ii) Wind: $r \to 0$, $v \to 0$ and $r \to \infty$, $v \to$ large.

(3)The adiabatic index(γ) chosen to : (a) $\gamma = \frac{4}{3}$, (ultra-relativistic) (b) $\gamma = \frac{5}{3}$ (non-relativistic) and (c) constant energy $\mathcal{E} = 0.01$ (+ positive).

The accretion and wind solutions with angular momentum.

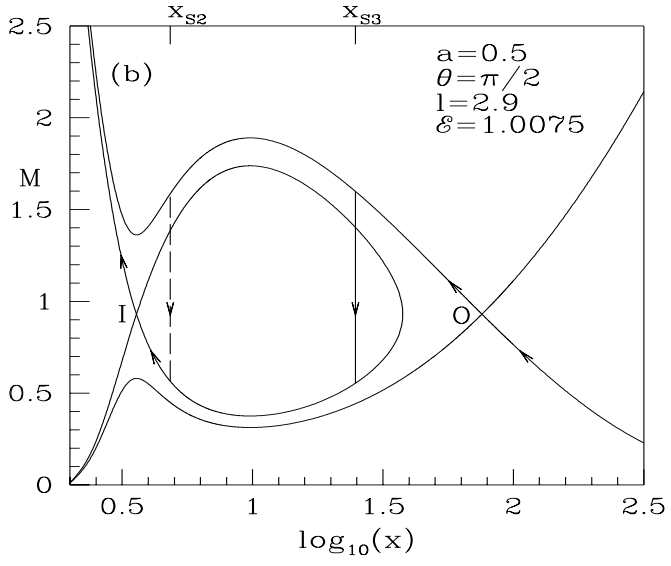

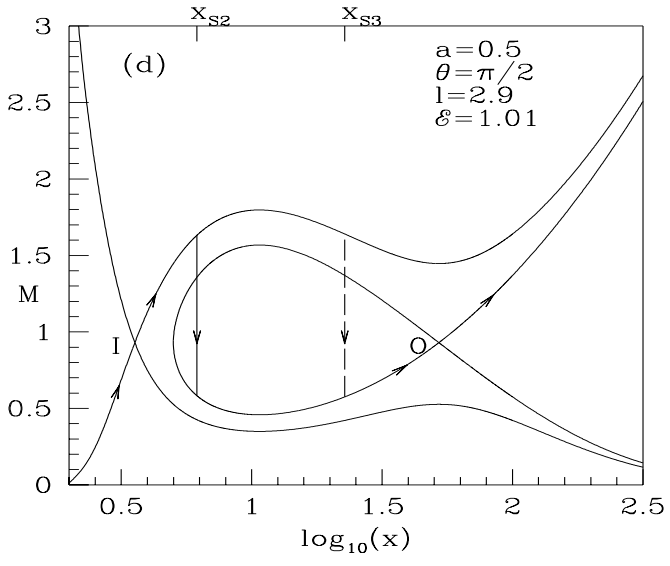

The solution topology (arrowed curve) includes a standing shocks in accretion and wind flows.

Ref: Mondal, Chakrabarti, MNRAS, 2006.

Flow topologies at various regions of the parameters space.

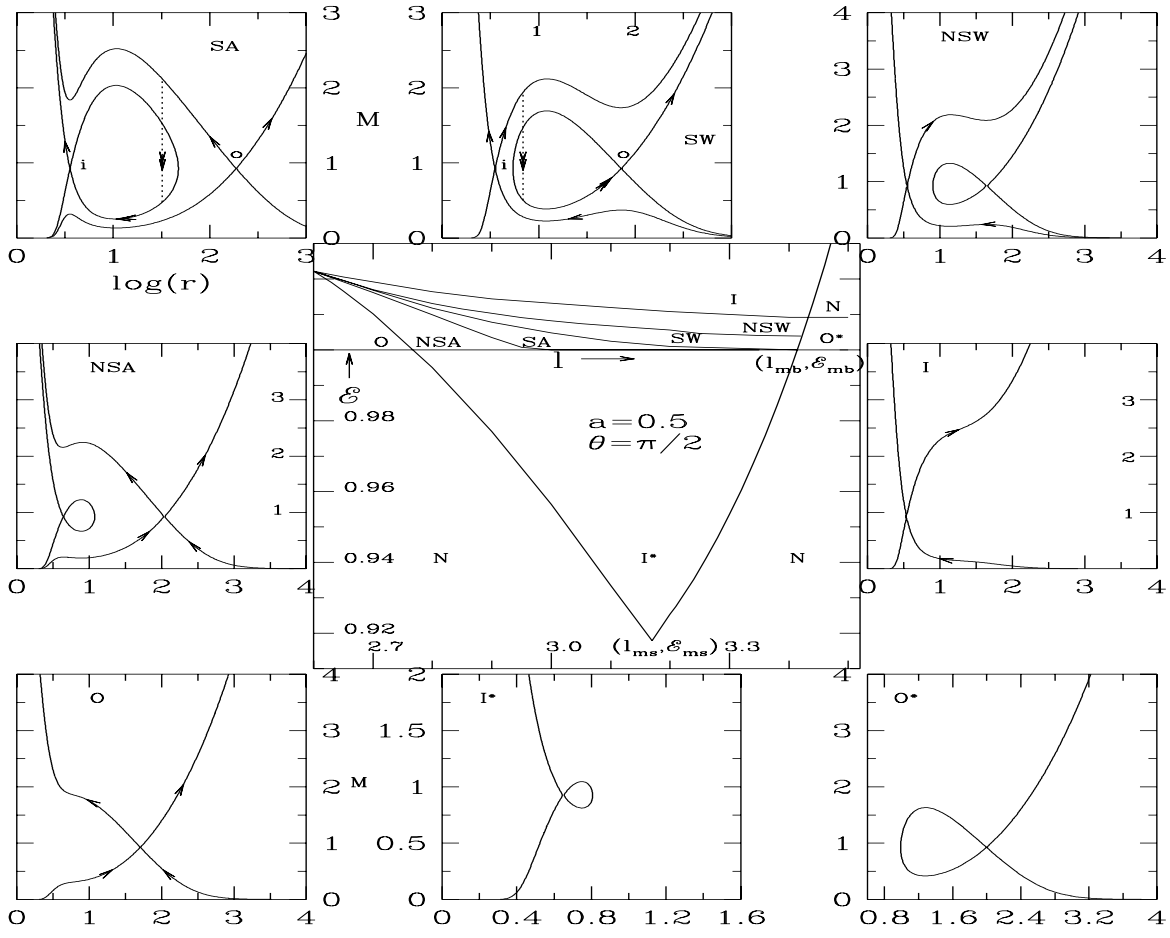

The region of the parameters space available standing and oscillating shocks.

Ref: Chakrabarti, MNRAS, 1996.

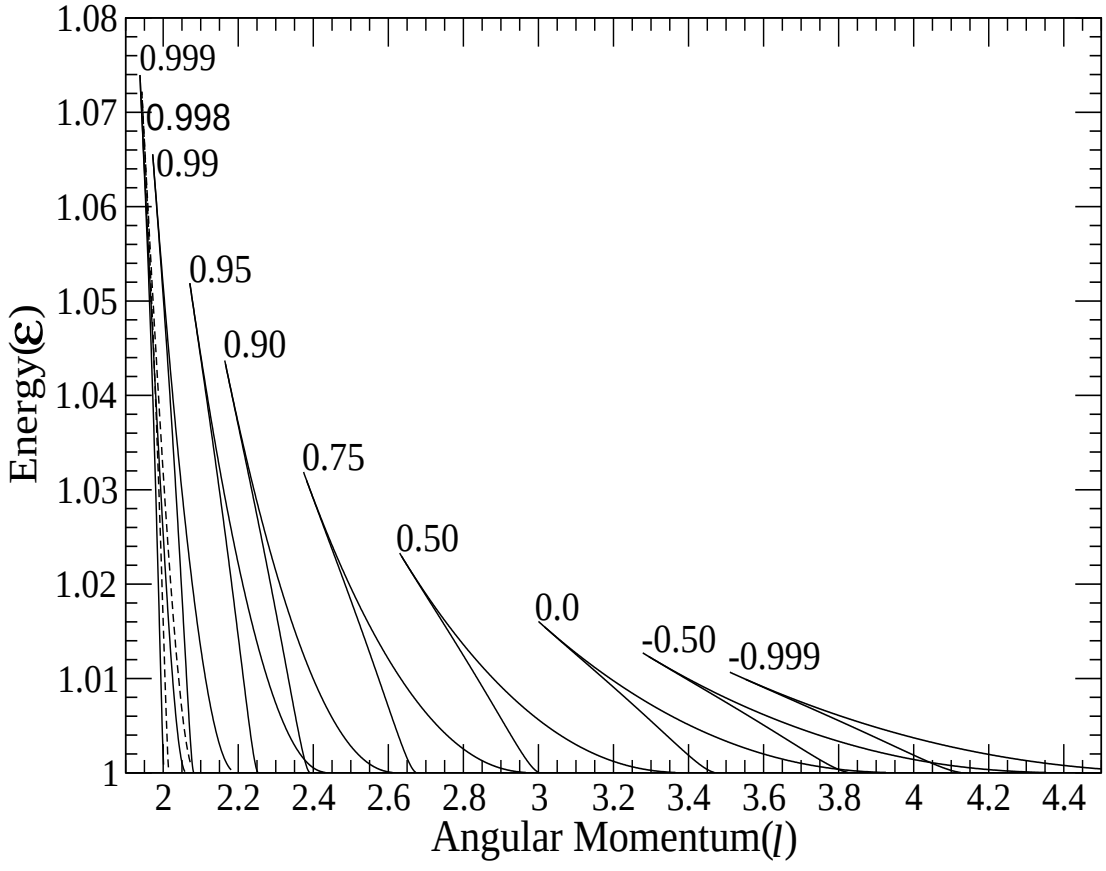

For $-1 < a < 1$, the parameters space responsible for the shocks in accretion flow.

Ref: Mondal, Apj, 2010.

Parameters space contains shocks in viscous accretion flow.

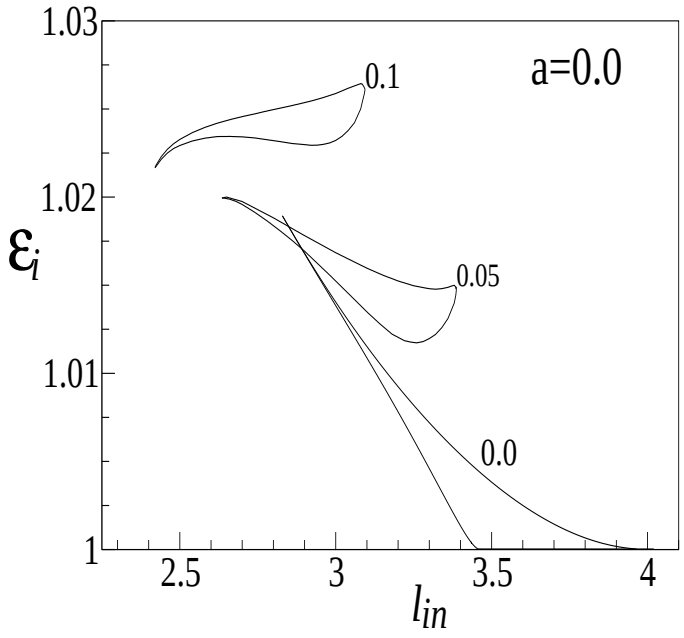

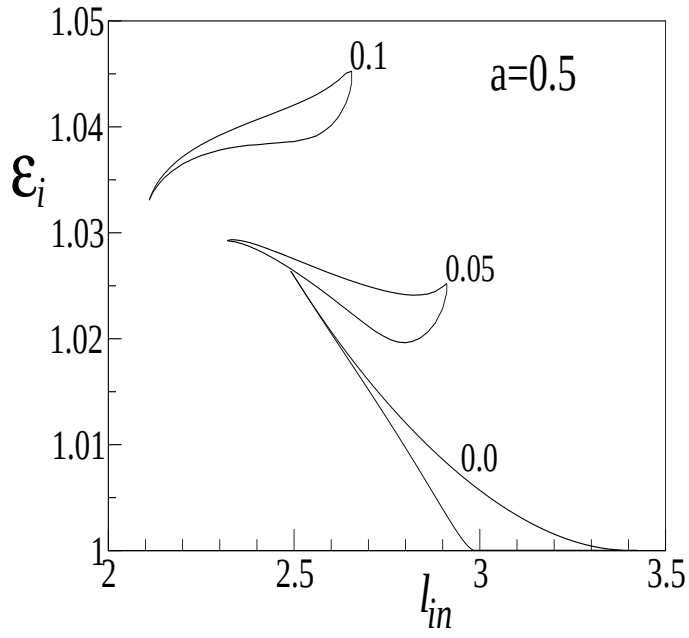

(1) With the increases of the viscosity parameter α_Π $(= 0.0, 0.05, 0.1)$, the different regions of the parameters space shrink and moved up to the high energy regions.

(2) The parameters space also shifts towards the region of lower angular momentum and higher energy with the increase of Kerr parameter while their overall-shape remain almost unchanged.

Ref: Mondal, Basu, and Chakrabarti, MNRAS, 2009.

SPH simulation produces shocks at different time steps :

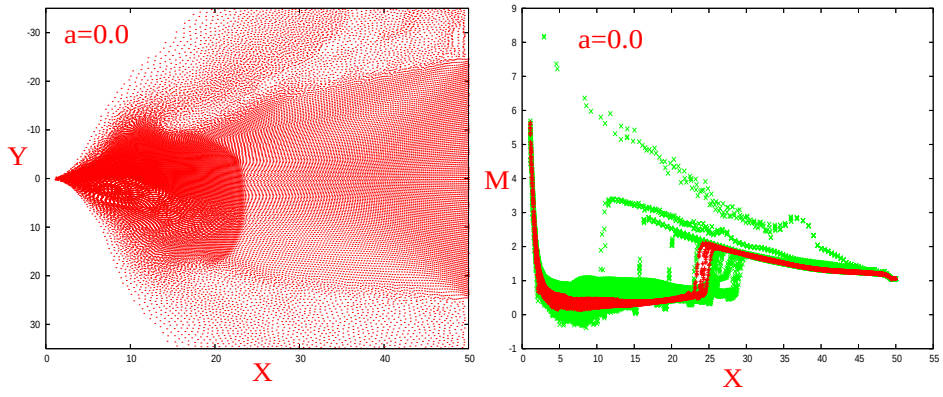

References:

Molteni, D., Lanzafame, G., & Chakrabarti, S. K. ApJ, 1994,

Molteni, D., Sponholz, H., & Chakrabarti, S. K. ApJ, 1996,

Ryu, D., Chakrabarti, S.K., & Molteni, D. ApJ, 1997.

SPH results are consistent with the analytic solution.

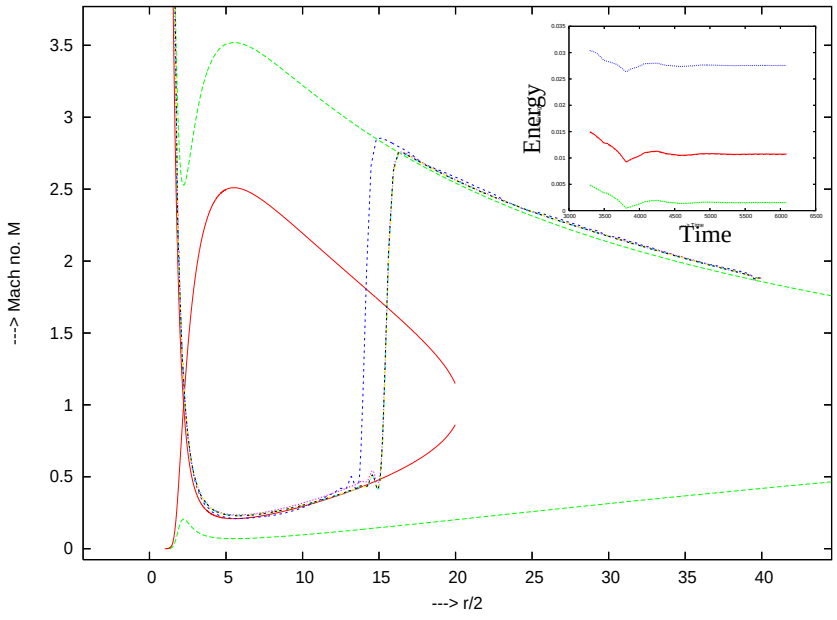

Accretion Flows Around Black Holes

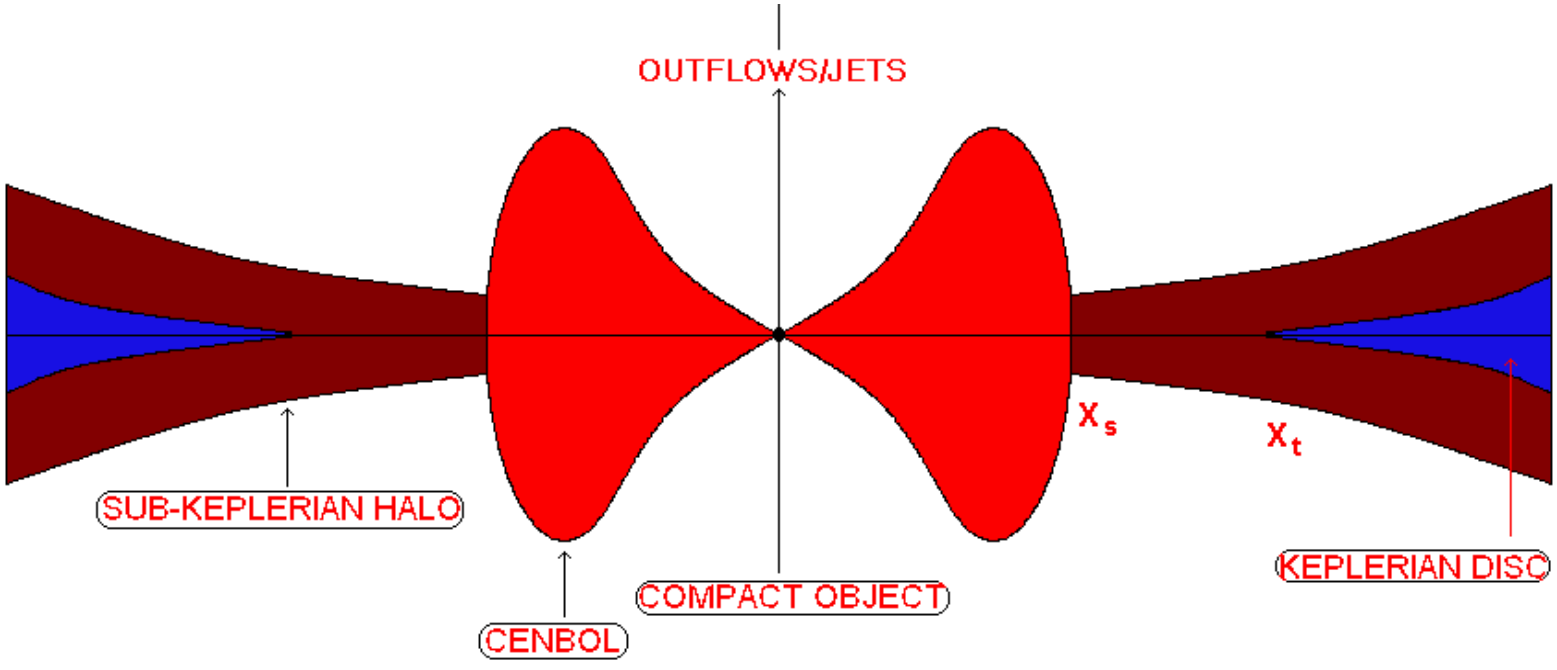

The importance of the shocks in the accretion flows :

- **The hot puffed up post-shock matter intercepts and inverse -Comptonizes a significant portion of the soft photons from the disk, to produce high energy power law tail.**
- **It produces non-thermal electrons through the shock acceleration, which is essential to explain the non-thermal power-law spectrum in high energy.**
- **The standing/oscillating shocks can explain the origin of QPOs and its time evolutions.**
- **The excess thermal gradient force in the post-shock drives a part of the incoming matter as outflow/jet along axis.**

References:
M. L. McConnell et al., 2002, ApJ, 572, 984
Ling & Wheaton, 2003, ApJ, 584, 399
Chakrabarti & Mandal, 2006, ApJ, 642, L49

(3): The accretion and wind solutions with variable adiabatic index (γ) ($\frac{4}{3} \leq \gamma \leq \frac{5}{3}$) and possibilities of shocks in the flow.

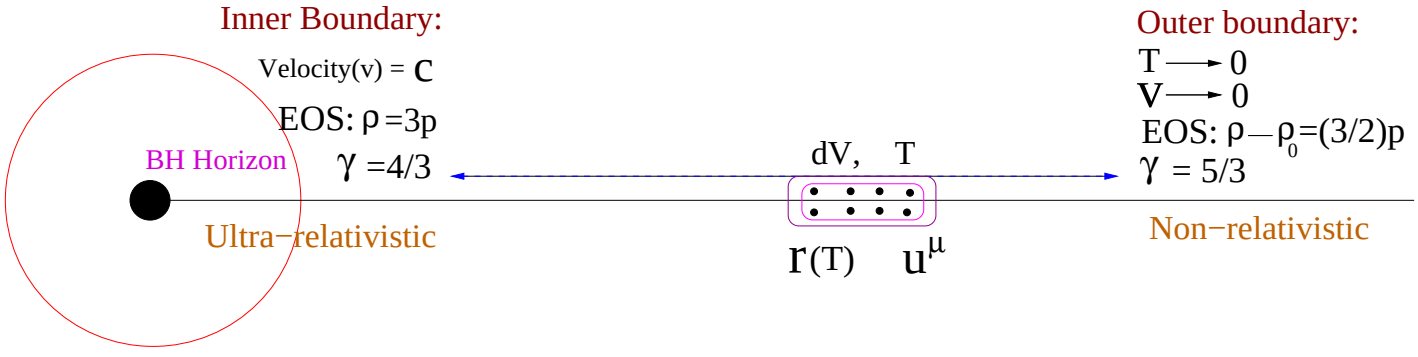

The probability distribution function.

Energy of a free particle $E = \sqrt{p^2c^2 + m^2c^4}$.

Therefore, the partition function is $Z = \frac{V}{h^3}\int_0^\infty e^{-\beta E}(4\pi p^2)dp = \frac{4\pi V}{h^3}\frac{K_2(\frac{mc^2}{k_BT})}{\left(\frac{mc^2}{k_BT}\right)}$

where K_2 is the modified Bessel's function of second kind.

The probability distribution function to the relativistic ideal gas is

(1) $$F(u/c)d(u/c) = \frac{\left(\frac{mc^2}{k_BT}\right)}{K_2\left(\frac{mc^2}{k_BT}\right)}(u/c)^2 \exp\left\{-\left(\frac{mc^2}{k_BT}\right)\sqrt{1+(u/c)^2}\right\}d(u/c).$$

References:

Synge, J. L. 1957, *The Relativistic Gas*

Chandrasekhar, S., 1939 *An introduction to the study of stellar structure*.

The relativistic EOS : $p = (\gamma - 1)(\rho - \rho_0)$.

The pressure p is the momentum flux through the unit area averaged over all the molecules, i.e., $p = \rho_0 < u^i v^i >$,

(2) $$p = \frac{1}{3}\rho_0(< u^0 > - < \frac{1}{u^0} >) = \frac{\rho_0 c^2}{\left(\frac{mc^2}{k_B T}\right)},$$

The total energy density ρ (kinetic+rest mass energy density) is related to ρ_0 as

(3) $$\rho = \rho_0 < u^0(\lambda) >= \rho_0 c^2 \left\{ \frac{3}{\left(\frac{mc^2}{k_B T}\right)} + K_1\left(\frac{mc^2}{k_B T}\right)/K_2\left(\frac{mc^2}{k_B T}\right) \right\},$$

where ρ_0 is rest mass density, $u^\mu = \frac{dx^\mu}{d\tau}$ and $v^i = \frac{dx^i}{dt}$.

Henceforth we choose $\lambda = \left(\frac{mc^2}{k_B T}\right)$ in our analysis.

The extreme limits: (1) Non-relativistic. (2) Ultra-relativistic.

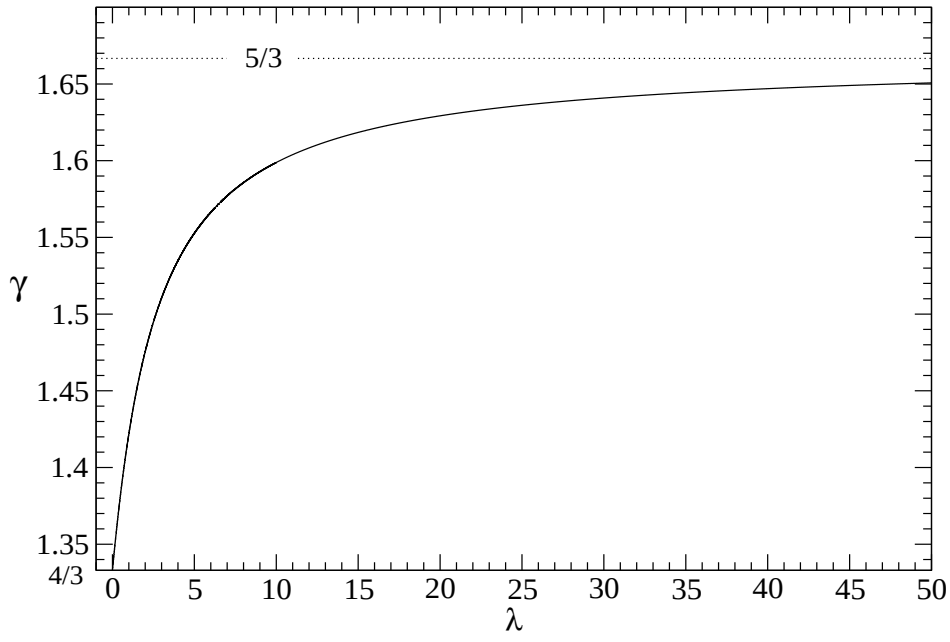

The adiabatic index γ ($\frac{4}{3} \leq \gamma \leq \frac{5}{3}$) is plotted w.r.t λ.

Verification of the sound speed limit: $a_s \leq 1/\sqrt{3}$.

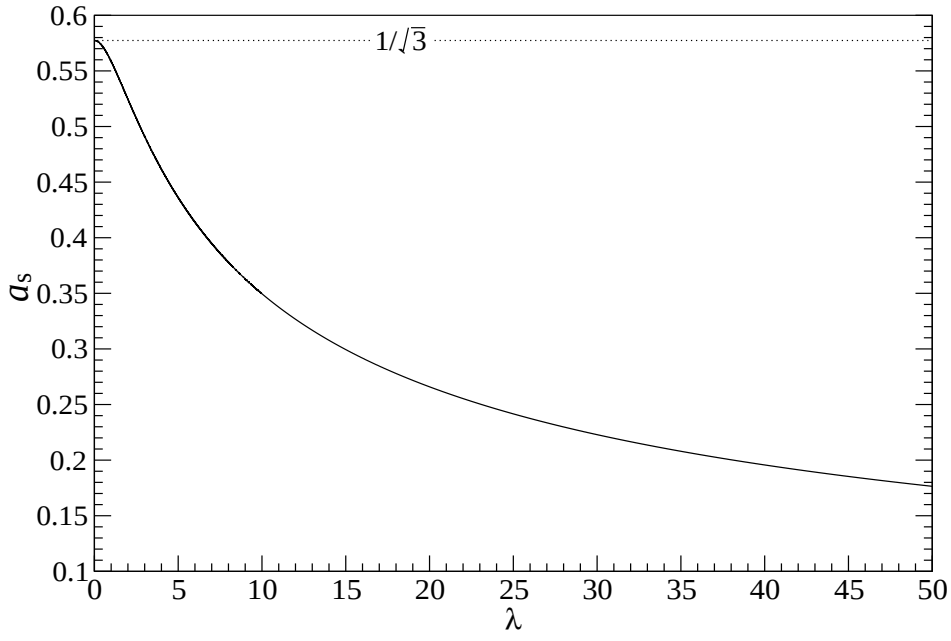

A plot of the sound speed a_s vs. λ is shown in figure.

The inequality, $a_s \leq 1/\sqrt{3}$ (0.57735) also satisfies.

The variation of adiabatic index (γ) with radius.

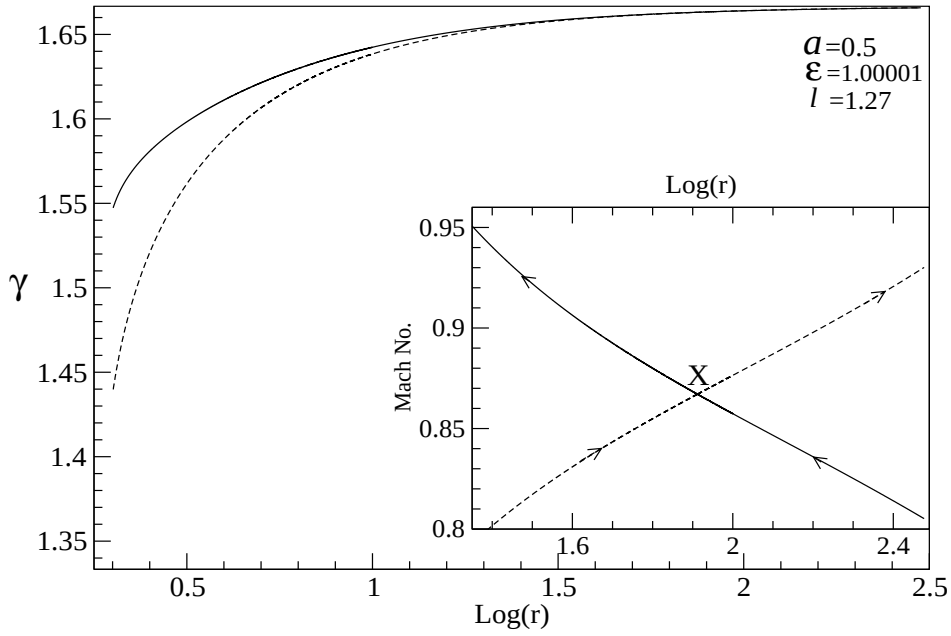

The variation γ as a function of radius is shown in the figure for both accretion (solid) and wind (dotted) flow topologies (in the sub-panel).

Note that the most of the flow topology contains one sonic point solution.

Ref: Mondal, Basu, CQG, 2011.

Number of sonic points in hydrodynamic flows.

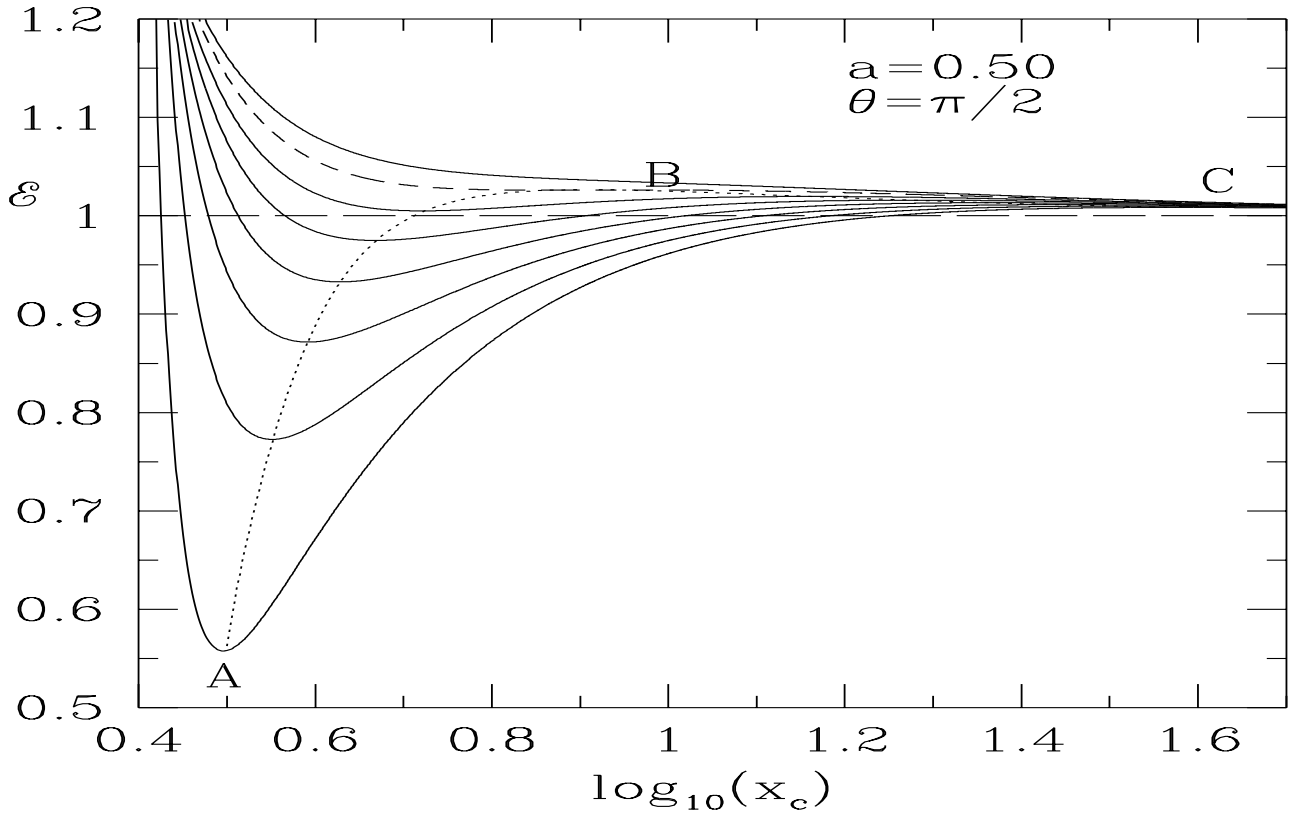

The curves are drawn for (top to bottom) $l =$ 2.3, 2.488, 2.7, 2.9, 3.1, 3.3, 3.5,3.7 respectively.

Results of previous study with $\gamma = \frac{4}{3}$ (ultra-relativistic).

Number of sonic points in hydrodynamic flows.

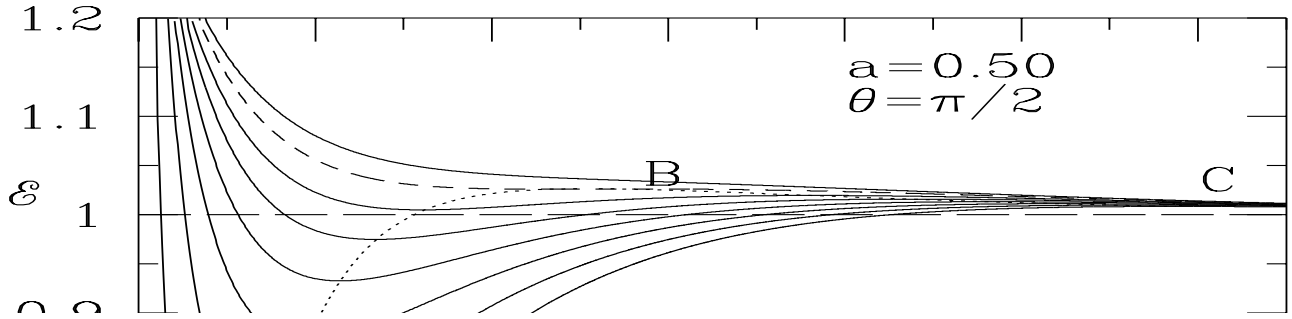

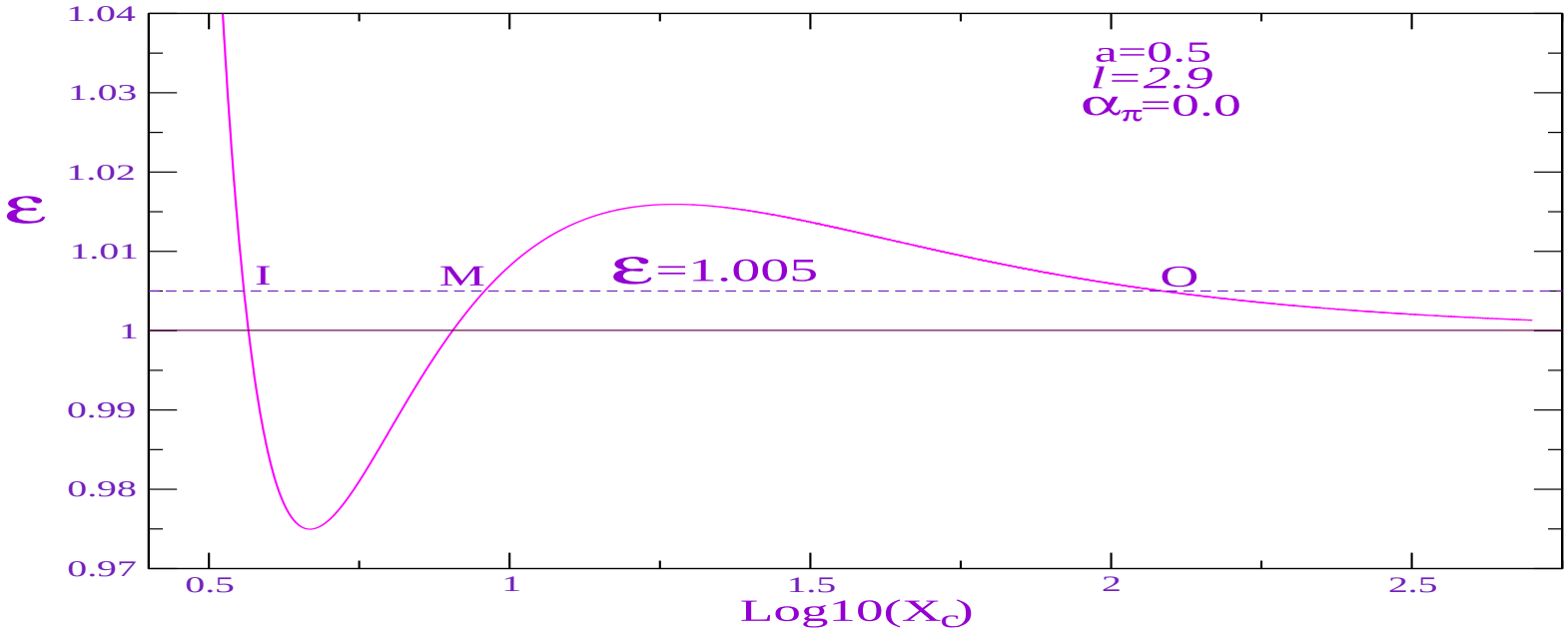

Results of previous study with $\gamma = \frac{4}{3}$ (ultra-relativistic).

Present study with variable adiabatic index ($\frac{4}{3} \leq \gamma \leq \frac{5}{3}$).

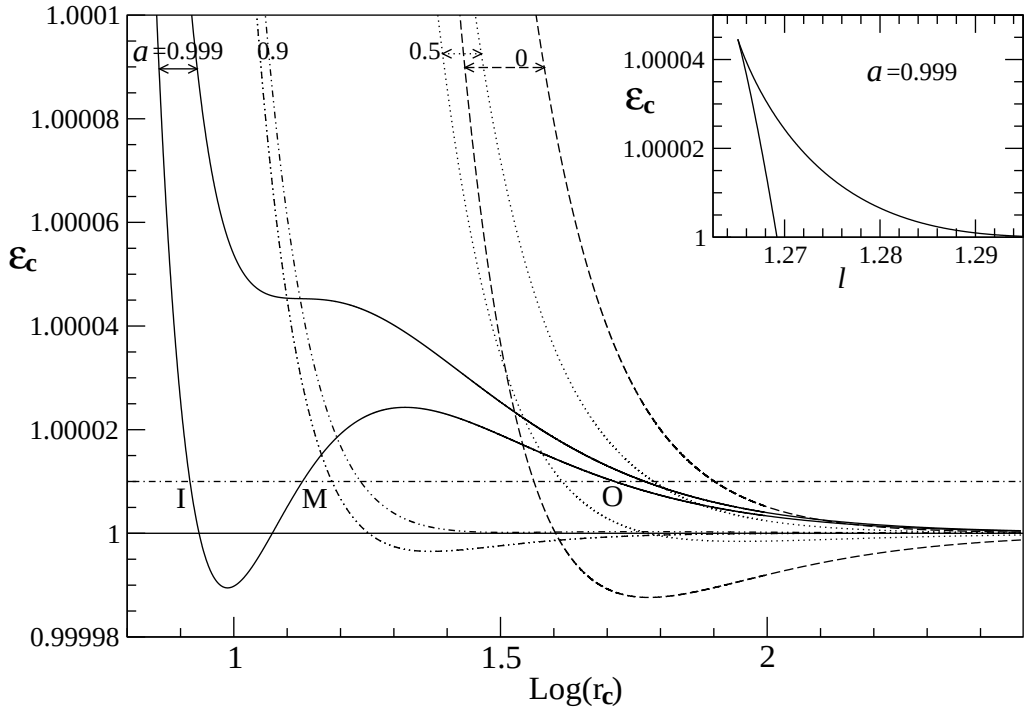

The variation $\mathcal{E}_c$ with r_c is shown for (a, l)=(0, 1.3)(top), (0, 1.4)(bottom), (0.5, 1.3)(top), (0.5, 1.33)(bottom), (0.9, 1.299)(top), (0.9, 1.301)(bottom), (0.999, 1.265)(top), (0.999, 1.27)(bottom). In the sub-panel a parameter space ($\mathcal{E}, l$) is also drawn when two saddle type ('X') critical points exist.

The variation γ with radius: a rare possibility.

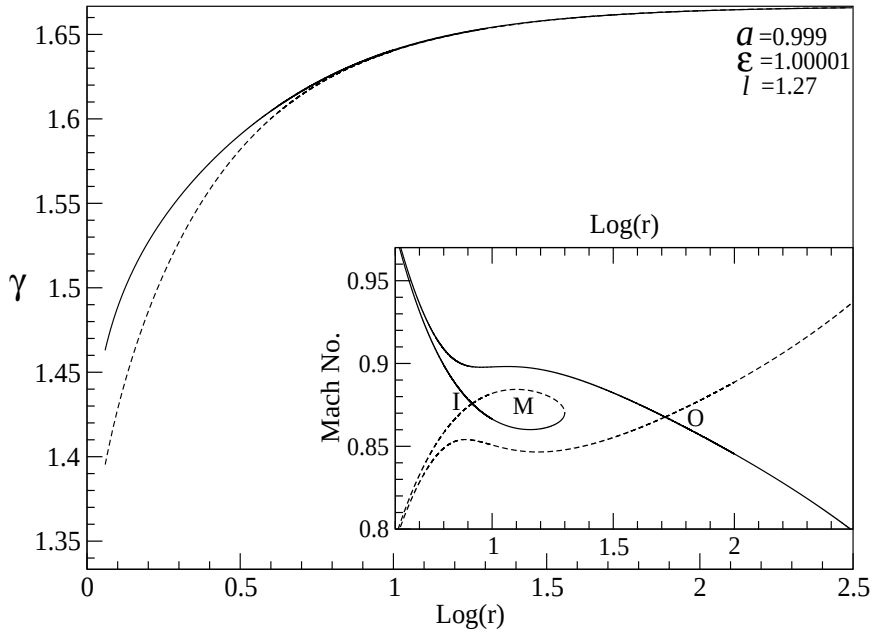

The variation γ as a function of radius is shown for different flow topologies when two saddle type ('X') critical points are present.

Important results and conclusions:

- In the relativistic equation of state, the adiabatic index γ is temperature dependent and changes from the non-relativistic to ultra -relativistic limit. As a result, from the outer edge to inner edge, γ varies continuously from $\frac{5}{3} \rightarrow \frac{4}{3}$.
- An artifact of constant ultra-relativistic value of $\gamma = \frac{4}{3}$ is that the flow has mostly two saddle('X')-type sonic points and may contain stable shocks if the shock conditions are satisfied in between two 'X'-type sonic points.
- However, we see that with the correct choice of EOS, up-to a distance very close to the critical point, γ does not change significantly from its non-relativistic value for both the accretion and winds. Therefore, the two 'X'-type sonic points becomes a rare possibility.

References:

- Mondal S., Basu P., 2011, *Classical Quantum Gravity,* 28 (2011) 235004.
- Basu P., Mondal S., 2013, Journal of New Astronomy, 694, 384
- Basu P., Mondal S. 2011, (astro-ph/1103-3330)
- Mondal S. 2010, APJ, 708 1442
- Chakrabarti S. K., 1996, MNRAS, 283, 325
- Chandrasekhar, S., 1939 *An introduction to the study of stellar structure* (Univ. of Chicago Press)
- Synge, J. L. 1957, *The Relativistic Gas* (Amsterdam: N.Holland)
- Falle, S. A. E. G., & Komissarov, S. S. 1996, MNRAS, 278, 586
- Sokolov, I., Zhang, H. M., & Sakai, J. I. 2001, J. Comput. Phys., 172, 209
- Tolman, R. C., 1934 *Relativity, Thermodynamics, and Cosmology* (Oxford: Clarendon Press)
- Wilson, J. R., & Mathews, G. J. 2003, *Relativistic Numerical Hydrodynamics*

THANK YOU.